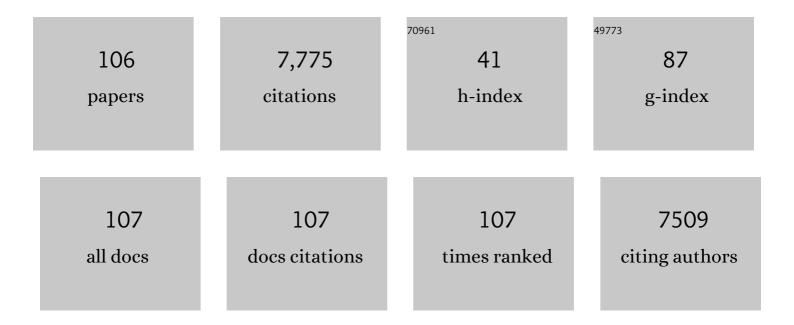


## List of Publications by Year in descending order

Source: https://exaly.com/author-pdf/2065902/publications.pdf

Version: 2024-02-01



OLL

#	Article	IF	CITATIONS
1	Post-illumination activity of Bi2WO6 in the dark from the photocatalytic "memory―effect. Journal of Advanced Ceramics, 2021, 10, 355-367.	8.9	48
2	Hydrous cerium oxides coated glass fiber for efficient and long-lasting arsenic removal from drinking water. Journal of Advanced Ceramics, 2021, 10, 247-257.	8.9	13
3	Self-Doping Surface Oxygen Vacancy-Induced Lattice Strains for Enhancing Visible Light-Driven Photocatalytic H <sub>2</sub> Evolution over Black TiO <sub>2</sub> . ACS Applied Materials & Interfaces, 2021, 13, 18758-18771.	4.0	127
4	Efficient oxygen reduction reaction by a highly porous, nitrogen-doped carbon sphere electrocatalyst through space confinement effect in nanopores. Journal of Advanced Ceramics, 2021, 10, 714-728.	8.9	33
5	Directing photocatalytic pathway to exceedingly high antibacterial activity in water by functionalizing holey ultrathin nanosheets of graphitic carbon nitride. Water Research, 2021, 198, 117125.	5.3	68
6	Photoirradiation-Induced Capacitance Enhancement in the <i>h</i> -WO <sub>3</sub> /Bi <sub>2</sub> WO <sub>6</sub> Submicron Rod Heterostructure under Simulated Solar Illumination and Its Postillumination Capacitance Enhancement Retainment from a Photocatalytic Memory Effect. ACS Applied Materials & amp; Interfaces, 2021, 13, 57214-57229.	4.0	16
7	Highly Selective, Defect-Induced Photocatalytic CO <sub>2</sub> Reduction to Acetaldehyde by the Nb-Doped TiO <sub>2</sub> Nanotube Array under Simulated Solar Illumination. ACS Applied Materials & Interfaces, 2020, 12, 55982-55993.	4.0	39
8	{001}/{101} facets co-exposed TiO2 microsheet arrays with Lanthanum doping for enhancing photocatalytic CO2 reduction. Journal of Materials Science: Materials in Electronics, 2020, 31, 19464-19474.	1.1	4
9	Direct Writing of Microfluidic Three-Dimensional Photonic Crystal Structures for Terahertz Technology Applications. ACS Applied Materials & Interfaces, 2019, 11, 41611-41616.	4.0	15
10	Mesoporous silica-protected silver nanoparticle disinfectant with controlled Ag <sup>+</sup> ion release, efficient magnetic separation, and effective antibacterial activity. Nanoscale Advances, 2019, 1, 840-848.	2.2	35
11	Direct-writing of vanadium dioxide/polydimethylsiloxane three-dimensional photonic crystals with thermally tunable terahertz properties. Journal of Materials Chemistry C, 2019, 7, 8185-8191.	2.7	9
12	Temperature-dependent photoluminescence and lasing properties of CsPbBr3 nanowires. Applied Physics Letters, 2019, 114, .	1.5	59
13	Modulation of terahertz properties of 3D ceramic photonic crystals via postâ€creation nonâ€metal anion doping treatment. Journal of the American Ceramic Society, 2019, 102, 4688-4697.	1.9	3
14	Internal Polarization Modulation in Bi <sub>2</sub> MoO <sub>6</sub> for Photocatalytic Performance Enhancement under Visible‣ight Illumination. ChemSusChem, 2018, 11, 1521-1532.	3.6	55
15	Photoinduced reversible lattice expansion in W-doped TiO2through the change of its electronic structure. Applied Physics Letters, 2018, 112, 061904.	1.5	4
16	Photocatalysis: a "Solar Sail―to Drive Microscale Objects in Water. Advanced Materials Technologies, 2018, 3, 1700384.	3.0	2
17	Postillumination Activity in a Single-Phase Photocatalyst of Mo-Doped TiO <sub>2</sub> Nanotube Array from Its Photocatalytic "Memory― ACS Sustainable Chemistry and Engineering, 2018, 6, 6166-6174.	3.2	47
18	Creation of 3D terahertz photonic crystals by the direct writing technique with a TiO <sub>2</sub>	1.9	16

#	Article	IF	CITATIONS
19	4D Printing of Complex Structures with a Fast Response Time to Magnetic Stimulus. ACS Applied Materials & Interfaces, 2018, 10, 36435-36442.	4.0	127
20	Synthesis of Bi <sub>2</sub> MoO <sub>6</sub> Nanosheets with Rich Oxygen Vacancies by Postsynthesis Etching Treatment for Enhanced Photocatalytic Performance. ACS Applied Nano Materials, 2018, 1, 3565-3578.	2.4	81
21	Anchoring Pd Nanoparticles on Fe <sub>3</sub> O <sub>4</sub> @SiO <sub>2</sub> Core–Shell Nanoparticles by Cross-Linked Polyvinylpyrrolidone for Nitrite Reduction. ACS Applied Nano Materials, 2018, 1, 5035-5043.	2.4	15
22	Direct Writing of Flexible Barium Titanate/Polydimethylsiloxane 3D Photonic Crystals with Mechanically Tunable Terahertz Properties. Advanced Optical Materials, 2017, 5, 1600977.	3.6	33
23	Creation of Pd/Al2O3 Catalyst by a Spray Process for Fixed Bed Reactors and Its Effective Removal of Aqueous Bromate. Scientific Reports, 2017, 7, 41797.	1.6	14
24	Large energy density in Ba doped Pb0.97La0.02(Zr0.65Sn0.3Ti0.05)O3 antiferroelectric ceramics with improved temperature stability. IEEE Transactions on Dielectrics and Electrical Insulation, 2017, 24, 744-748.	1.8	17
25	Nanocomposites: Highâ€Energyâ€Density Dielectric Polymer Nanocomposites with Trilayered Architecture (Adv. Funct. Mater. 20/2017). Advanced Functional Materials, 2017, 27, .	7.8	4
26	Highâ€Energyâ€Density Dielectric Polymer Nanocomposites with Trilayered Architecture. Advanced Functional Materials, 2017, 27, 1606292.	7.8	338
27	Biocompatible and Flexible Hydrogel Diodeâ€Based Mechanical Energy Harvesting. Advanced Materials Technologies, 2017, 2, 1700118.	3.0	29
28	Highâ€Performance Polymers Sandwiched with Chemical Vapor Deposited Hexagonal Boron Nitrides as Scalable Highâ€Temperature Dielectric Materials. Advanced Materials, 2017, 29, 1701864.	11.1	270
29	Flexible Ionic Diodes for Lowâ€Frequency Mechanical Energy Harvesting. Advanced Energy Materials, 2017, 7, 1601983.	10.2	51
30	Selfâ€Healable Polymer Nanocomposites Capable of Simultaneously Recovering Multiple Functionalities. Advanced Functional Materials, 2016, 26, 3524-3531.	7.8	69
31	Towards multicaloric effect with ferroelectrics. Physical Review B, 2016, 94, .	1.1	33
32	Effect of Mn <sub>3</sub> O <sub>4</sub> nanoparticle composition and distribution on graphene as a potential hybrid anode material for lithium-ion batteries. RSC Advances, 2016, 6, 33022-33030.	1.7	19
33	In situ growth of TiO <sub>2</sub> on TiN nanoparticles for non-noble-metal plasmonic photocatalysis. RSC Advances, 2016, 6, 72659-72669.	1.7	36
34	Sandwich-structured polymer nanocomposites with high energy density and great charge–discharge efficiency at elevated temperatures. Proceedings of the National Academy of Sciences of the United States of America, 2016, 113, 9995-10000.	3.3	317
35	Self-suspended polyaniline containing self-dissolved lyotropic liquid crystal with electrical conductivity. Journal of Polymer Science Part A, 2016, 54, 3578-3582.	2.5	4
36	Post-illumination activity of SnO2 nanoparticle-decorated Cu2O nanocubes by H2O2 production in dark from photocatalytic "memory― Scientific Reports, 2016, 6, 20878.	1.6	40

Qi Li

#	Article	IF	CITATIONS
37	Toward Wearable Cooling Devices: Highly Flexible Electrocaloric Ba <sub>0.67</sub> Sr <sub>0.33</sub> TiO <sub>3</sub> Nanowire Arrays. Advanced Materials, 2016, 28, 4811-4816.	11.1	101
38	Enhanced visible light adsorption of heavily nitrogen doped TiO2 thin film via ion beam assisted deposition. Journal of Materials Science: Materials in Electronics, 2016, 27, 2968-2973.	1.1	2
39	Synthesis of Superparamagnetic Core–Shell Structure Supported Pd Nanocatalysts for Catalytic Nitrite Reduction with Enhanced Activity, No Detection of Undesirable Product of Ammonium, and Easy Magnetic Separation Capability. ACS Applied Materials & Interfaces, 2016, 8, 2035-2047.	4.0	25
40	A Hybrid Material Approach Toward Solutionâ€Processable Dielectrics Exhibiting Enhanced Breakdown Strength and High Energy Density. Advanced Functional Materials, 2015, 25, 3505-3513.	7.8	152
41	Highâ€Energy Storage Performance of (Pb <sub>0.87</sub> Ba <sub>0.1</sub> La <sub>0.02</sub> )(Zr <sub>0.68</sub> Sn <sub>0.24</sub> Ti <sub>0.0 Antiferroelectric Ceramics Fabricated by the Hotâ€Press Sintering Method. Journal of the American Ceramic Society. 2015. 98. 1175-1181.</sub>	8)C	) <sub>3168</sub>
42	Real time, in situ observation of the photocatalytic inactivation of Saccharomyces cerevisiae cells. Materials Science and Engineering C, 2015, 49, 75-83.	3.8	2
43	Relaxor Ferroelectricâ€Based Electrocaloric Polymer Nanocomposites with a Broad Operating Temperature Range and High Cooling Energy. Advanced Materials, 2015, 27, 2236-2241.	11.1	143
44	Flexible high-temperature dielectric materials from polymer nanocomposites. Nature, 2015, 523, 576-579.	13.7	1,476
45	Colossal Room-Temperature Electrocaloric Effect in Ferroelectric Polymer Nanocomposites Using Nanostructured Barium Strontium Titanates. ACS Nano, 2015, 9, 7164-7174.	7.3	164
46	Superior As( <scp>iii</scp> ) removal performance of hydrous MnOOH nanorods from water. RSC Advances, 2015, 5, 53280-53288.	1.7	40
47	Efficient photocatalytic removal of aqueous NH4+–NH3 by palladium-modified nitrogen-doped titanium oxide nanoparticles under visible light illumination, even in weak alkaline solutions. Chemical Engineering Journal, 2015, 264, 728-734.	6.6	43
48	Electrocaloric Effect: Relaxor Ferroelectricâ€Based Electrocaloric Polymer Nanocomposites with a Broad Operating Temperature Range and High Cooling Energy (Adv. Mater. 13/2015). Advanced Materials, 2015, 27, 2267-2267.	11.1	2
49	Synthesis of Mn <sub>3</sub> O <sub>4</sub> /CeO <sub>2</sub> Hybrid Nanotubes and Their Spontaneous Formation of a Paper-like, Free-Standing Membrane for the Removal of Arsenite from Water. ACS Applied Materials & Interfaces, 2015, 7, 26291-26300.	4.0	41
50	NiO hierarchical hollow nanofibers as high-performance supercapacitor electrodes. RSC Advances, 2015, 5, 96205-96212.	1.7	47
51	Anti-algal activity of palladium oxide-modified nitrogen-doped titanium oxide photocatalyst on Anabaena sp. PCC 7120 and its photocatalytic degradation on Microcystin LR under visible light illumination. Chemical Engineering Journal, 2015, 264, 437-444.	6.6	18
52	Solution-processed ferroelectric terpolymer nanocomposites with high breakdown strength and energy density utilizing boron nitride nanosheets. Energy and Environmental Science, 2015, 8, 922-931.	15.6	541
53	Real Time, in situ Observation of the Photocatalytic Destruction of Saccharomyces cerevisiae Cells by Palladium-modified Nitrogen-doped Titanium Oxide Thin Film. Journal of Materials Science and Technology, 2015, 31, 48-54.	5.6	4
54	Nanostructured Visible-Light Photocatalysts for Water Purification. , 2014, , 297-317.		5

#	Article	IF	CITATIONS
55	Energy Storage: High Energy and Power Density Capacitors from Solutionâ€Processed Ternary Ferroelectric Polymer Nanocomposites (Adv. Mater. 36/2014). Advanced Materials, 2014, 26, 6356-6356.	11.1	4
56	PdO loaded TiO2 hollow sphere composite photocatalyst with a high photocatalytic disinfection efficiency on bacteria. Chemical Engineering Journal, 2014, 249, 63-71.	6.6	23
57	Passivated n–p co-doping of niobium and nitrogen into self-organized TiO2 nanotube arrays for enhanced visible light photocatalytic performance. Applied Catalysis B: Environmental, 2014, 144, 343-352.	10.8	37
58	High Energy and Power Density Capacitors from Solutionâ€Processed Ternary Ferroelectric Polymer Nanocomposites. Advanced Materials, 2014, 26, 6244-6249.	11.1	448
59	Synthesis of a superparamagnetic MFNs@SiO <sub>2</sub> @Ag <sub>4</sub> SiW <sub>12</sub> O <sub>40</sub> /Ag composite photocatalyst, its superior photocatalytic performance under visible light illumination, and its easy magnetic separation. RSC Advances. 2014. 4. 30090-30099.	1.7	10
60	Ionic Potential: A General Material Criterion for the Selection of Highly Efficient Arsenic Adsorbents. Journal of Materials Science and Technology, 2014, 30, 949-953.	5.6	20
61	Template-free solvothermal synthesis of WO <sub>3</sub> /WO <sub>3</sub> ·H <sub>2</sub> O hollow spheres and their enhanced photocatalytic activity from the mixture phase effect. CrystEngComm, 2014, 16, 7493-7501.	1.3	59
62	Suppression of energy dissipation and enhancement of breakdown strength in ferroelectric polymer–graphene percolative composites. Journal of Materials Chemistry C, 2013, 1, 7034.	2.7	78
63	Antifungal Activity and Mechanism of Palladium-Modified Nitrogen-Doped Titanium Oxide Photocatalyst on Agricultural Pathogenic Fungi <i>Fusarium graminearum</i> . ACS Applied Materials & Interfaces, 2013, 5, 10953-10959.	4.0	75
64	Well-dispersed, ultrasmall, superparamagnetic magnesium ferrite nanocrystallites with controlled hydrophilicity/hydrophobicity and high saturation magnetization. RSC Advances, 2013, 3, 13961.	1.7	13
65	Exceptional arsenic (III,V) removal performance of highly porous, nanostructured ZrO2 spheres for fixed bed reactors and the full-scale system modeling. Water Research, 2013, 47, 6258-6268.	5.3	99
66	Mg-doping: a facile approach to impart enhanced arsenic adsorption performance and easy magnetic separation capability to α-Fe <sub>2</sub> O <sub>3</sub> nanoadsorbents. Journal of Materials Chemistry A, 2013, 1, 830-836.	5.2	57
67	Highly efficient catalytic reduction of bromate in water over a quasi-monodisperse, superparamagnetic Pd/Fe3O4 catalyst. Journal of Materials Chemistry A, 2013, 1, 9215.	5.2	46
68	Fluorineâ€Free Synthesis of Wellâ€Dispersed Hollow <scp><scp>TiO</scp></scp> <sub>2</sub> Spheres via Ostwald Ripening: Process, Mechanism, and Photocatalytic Performance. Journal of the American Ceramic Society, 2013, 96, 1421-1427.	1.9	17
69	As(III) and As(V) Adsorption by Hydrous Zirconium Oxide Nanoparticles Synthesized by a Hydrothermal Process Followed with Heat Treatment. Industrial & Engineering Chemistry Research, 2012, 51, 353-361.	1.8	95
70	The synthesis of nitrogen/sulfur co-doped TiO2 nanocrystals with a high specific surface area and a high percentage of {001} facets and their enhanced visible-light photocatalytic performance. Nanoscale Research Letters, 2012, 7, 590.	3.1	35
71	Synthesis and Characterization of Niobium-doped TiO2 Nanotube Arrays by Anodization of Ti–20Nb Alloys. Journal of Materials Science and Technology, 2012, 28, 865-870.	5.6	31
72	Exceptional arsenic adsorption performance of hydrous cerium oxide nanoparticles: Part B. Integration with silica monoliths and dynamic treatment. Chemical Engineering Journal, 2012, 185-186, 136-143.	6.6	36

#	Article	IF	CITATIONS
73	Exceptional arsenic adsorption performance of hydrous cerium oxide nanoparticles: Part A. Adsorption capacity and mechanism. Chemical Engineering Journal, 2012, 185-186, 127-135.	6.6	182
74	High efficient As(III) removal by self-assembled zinc oxide micro-tubes synthesized by a simple precipitation process. Journal of Materials Science, 2011, 46, 5851-5858.	1.7	23
75	Enhanced Photocatalytic Disinfection of Escherichia coli Bacteria by Silver and Nickel Comodification of a Nitrogenâ€Doped Titanium Oxide Nanoparticle Photocatalyst Under Visible‣ight Illumination. Journal of the American Ceramic Society, 2010, 93, 531-535.	1.9	5
76	Enhanced Photocatalytic Disinfection of <i>Escherichia coli</i> Bacteria by Silver Modification of Nitrogenâ€Doped Titanium Oxide Nanoparticle Photocatalyst Under Visibleâ€Light Illumination. Journal of the American Ceramic Society, 2010, 93, 3880-3885.	1.9	16
77	Heavily Nitrogenâ€Doped Titanium Oxide Thin Films by Reactive Sputtering and Excimer Laser Annealing. Journal of the American Ceramic Society, 2010, 93, 3039-3042.	1.9	1
78	Enhanced photocatalytic disinfection of microorganisms by transition-metal-ion-modification of nitrogen-doped titanium oxide. Journal of Materials Research, 2010, 25, 167-176.	1.2	15
79	As(III) removal by hydrous titanium dioxide prepared from one-step hydrolysis of aqueous TiCl4 solution. Water Research, 2010, 44, 5713-5721.	5.3	109
80	Composite Photocatalyst of Nitrogen and Fluorine Codoped Titanium Oxide Nanotube Arrays with Dispersed Palladium Oxide Nanoparticles for Enhanced Visible Light Photocatalytic Performance. Environmental Science & Technology, 2010, 44, 3493-3499.	4.6	43
81	Memory antibacterial effect from photoelectron transfer between nanoparticles and visible light photocatalyst. Journal of Materials Chemistry, 2010, 20, 1068-1072.	6.7	60
82	Nanostructured Visible-Light Photocatalysts for Water Purification. , 2009, , 17-37.		4
83	As(III) Removal by Palladium-Modified Nitrogen-Doped Titanium Oxide Nanoparticle Photocatalyst. Environmental Science & Technology, 2009, 43, 1534-1539.	4.6	56
84	Self-Organized Nitrogen and Fluorine Co-doped Titanium Oxide Nanotube Arrays with Enhanced Visible Light Photocatalytic Performance. Environmental Science & Technology, 2009, 43, 8923-8929.	4.6	82
85	Electronic band structures of TiO2 with heavy nitrogen doping. Journal Wuhan University of Technology, Materials Science Edition, 2008, 23, 799-803.	0.4	3
86	Palladium Oxide Nanoparticles on Nitrogenâ€Doped Titanium Oxide: Accelerated Photocatalytic Disinfection and Postâ€Illumination Catalytic "Memory― Advanced Materials, 2008, 20, 3717-3723.	11.1	166
87	Inverse Opal Structure of Nitrogen-Doped Titanium Oxide with Enhanced Visible-Light Photocatalytic Activity. Journal of the American Ceramic Society, 2008, 91, 660-663.	1.9	31
88	Enhanced Visible Light Absorption in a Photocatalytic Thin Film from a Decoupled Photonic Crystal. Journal of the American Ceramic Society, 2008, 91, 2575-2580.	1.9	4
89	Heavily Nitrogenâ€Doped Dualâ€Phase Titanium Oxide Thin Films by Reactive Sputtering and Rapid Thermal Annealing. Journal of the American Ceramic Society, 2008, 91, 3167-3172.	1.9	26
90	Treatment of Coliphage MS2 with Palladium-Modified Nitrogen-Doped Titanium Oxide Photocatalyst Illuminated by Visible Light. Environmental Science & Technology, 2008, 42, 6148-6153.	4.6	69

#	Article	IF	CITATIONS
91	Enhanced visible-light absorption from PdO nanoparticles in nitrogen-doped titanium oxide thin films. Applied Physics Letters, 2007, 90, 063109.	1.5	51
92	Modulation of MS2 virus adsorption on TiO2semiconductor film by nitrogen doping. Journal of Materials Research, 2007, 22, 3036-3041.	1.2	4
93	Enhanced Visible-Light-Induced Photocatalytic Disinfection ofE. coliby Carbon-Sensitized Nitrogen-Doped Titanium Oxide. Environmental Science & Technology, 2007, 41, 5050-5056.	4.6	139
94	Effect of Precursor Ratio on Synthesis and Optical Absorption of TiON Photocatalytic Nanoparticles. Journal of the American Ceramic Society, 2007, 90, 1045-1050.	1.9	24
95	Enhanced Visible-Light Photocatalytic Degradation of Humic Acid by Palladium-Modified Nitrogen-Doped Titanium Oxide. Journal of the American Ceramic Society, 2007, 90, 070916223044002-???.	1.9	16
96	Nonlinear Elasticity and Yielding of Nanoparticle Glasses. Langmuir, 2006, 22, 2441-2443.	1.6	23
97	Microwave Bandgap in Multilayer Ceramic Structures. Journal of the American Ceramic Society, 2006, 89, 1087-1090.	1.9	1
98	Ordered Ceramic Microstructures from Butterfly Bio-template. Journal of the American Ceramic Society, 2006, 89, 060427083300014-???.	1.9	14
99	Strong Suppression and Enhancement of Photoluminescence in Zn2SiO4:Mn2+ Inverse Opal Photonic Crystals. Journal of the American Ceramic Society, 2006, 89, 060427083300027-???.	1.9	6
100	Planar MgB2 superconductor-normal metal-superconductor Josephson junctions fabricated using epitaxial MgB2â^•TiB2 bilayers. Applied Physics Letters, 2006, 88, 222511.	1.5	29
101	Poly(acrylic acid)-Poly(ethylene oxide) Comb Polymer Effects on BaTiO3Nanoparticle Suspension Stability. Journal of the American Ceramic Society, 2004, 87, 181-186.	1.9	116
102	Photonic structures in butterflyThaumantis diores. Science Bulletin, 2004, 49, 2545-2546.	1.7	0
103	Synthesis of (Pb,La)(Zr,Ti)O <sub>3</sub> Inverse Opal Photonic Crystals. Journal of the American Ceramic Society, 2003, 86, 867-869.	1.9	20
104	Critical current density and resistivity of MgB2 films. Applied Physics Letters, 2003, 83, 102-104.	1.5	75
105	Photonic band gap in (Pb,La)(Zr,Ti)O3 inverse opals. Applied Physics Letters, 2003, 82, 3617-3619.	1.5	26
106	Role of strain in magnetotransport properties of Pr0.67Sr0.33MnO3 thin films. Journal of Applied Physics, 2000, 87, 7409-7414.	1.1	88